Spectrochimica Acta Part A: Molecular and Biomolecular Spectroscopy 163 (2016) 68–72

Contents lists available at ScienceDirect

Spectrochimica Acta Part A: Molecular and Biomolecular Spectroscopy

journal homepage: www.elsevier.com/locate/saa

SERS spectrum of gallic acid obtained from a modified silver colloid

C. Garrido [a,*], G. Diaz-Fleming [b], M.M. Campos-Vallette [a]

[a] Laboratory of Vibrational Spectroscopy, Department of Chemistry, Faculty of Sciences, Universidad de Chile, Santiago, Chile
[b] Laboratory of Molecular and Atomic Spectroscopy, Department of Chemistry, Faculty of Sciences, Universidad de Playa Ancha, Valparaíso, Chile

ARTICLE INFO

Article history:
Received 2 January 2016
Received in revised form 8 March 2016
Accepted 20 March 2016
Available online 22 March 2016

Keywords:
Gallic acid
DFT quantum chemical calculations
SERS
Modified silver colloid

ABSTRACT

Two different crystals of the gallic acid were microscopically separated from a p.a. commercial product. The Raman spectra analysis allowed distinguishing monomeric and dimeric structures. The vibrational wave numbers were computed using DFT quantum chemical calculations. The data obtained from wave number calculations are used to assign vibrational bands obtained in the Raman spectrum. The dimer, characterized as ellagic acid, involves the carboxyl and hydroxyl moieties. The Raman spectrum in water solution of each species is dominated by the monomeric form. A low negatively charged Ag colloid allowed obtain to the best of our knowledge, the first surface enhanced Raman scattering (SERS) spectrum of the gallic acid. The possible electrophilic attacking sites of the title molecule are identified using MEP surface plot study and the orientation of the analyte on the metal surface is proposed tilted to the surface.

1. Introduction

Iron gall inks have been deeply investigated in relation to the observed degradation in patrimonial artworks probably due to their corrosive nature and color instability [1]; in particular, Raman data for historic iron gall inks are not easy to obtain, although M. Leona et al. [2] used the surface-enhanced Raman scattering (SERS) technique to identify several natural dyes and other chemicals in artworks; however, no SERS data were provided for gallic acid (GA). For GA, Alvarez-Ros et al. [3] points out that chemical changes, such as ring opening and or polymerization of aromatic rings, undergone when this molecule is deposited onto a colloidal silver surface. Actually, the catalytic activity of metal surfaces on distinct reactions has been widely recognized [4,5]. As a matter of fact, the high electron density of this molecule within atoms carrying lone electron pairs, make difficult the approach of that analyte to a colloidal metal surface, thus avoiding to obtain a proper SERS spectrum. A recent publication of our research group concerns the fabrication and use of a low charged Ag colloid giving promising results into obtaining SERS spectrum of large-electron systems [6]. The purpose of the present work is to obtain the SERS spectrum of the gallic acid using this modified Ag colloid.

The reliability of the SERS data is considered by comparison with the normal Raman spectrum. The orientation of the analyte is inferred from the observed intensity and wavenumber shifts relative to the Raman spectrum, by using the SERS selection rules [7] indicating that modes having their Raman polarizability *z*-component perpendicular to the surface are likely to become more enhanced than the parallel ones. In order to interpret the SERS effect, theoretical considerations must be taken into account. In this respect, two complementary components of enhancement in SERS have been pointed out [8]: Electromagnetic (EM) and Charge Transfer (CT). The first one mainly arises from the coupling of light with the plasmons on metal the surface, driving its subsequent excitation. The CT mechanism involves molecular interactions between the metal surface and the adsorbate, increasing its molecular polarizability. The CT mechanism produce less SERS enhancement that the EM component and drives shifts in selected Raman fundamentals. The charge transfer mechanism is restricted by its nature to molecules directly adsorbed on the metal, as opposed to the electromagnetic effect, which extends to certain distance beyond the surface. For the correct interpretation of the SERS data, it is necessary to have, as a guideline, a proper vibrational assignment of the Raman spectrum, which will be theoretical assisted in the present work by using density functional theory (DFT) [9], which has come up in the last years as an inviting and economical alternative to the conventional ab initio methods. DFT proved its ability in reproducing various molecular properties, including vibrational spectra, optimized geometry and molecular electrostatic potential (MEP), the latter being useful to support the orientation of the molecule on the surface deducted from the SERS selection rules. Recently, J. Huguenin et al [10] studied the deprotonation of the gallic

* Corresponding author.
E-mail address: cgarridoleiva@ug.uchile.cl (C. Garrido).

http://dx.doi.org/10.1016/j.saa.2016.03.028
1386-1425/

acid at several pH using Raman data thus obtaining information on the pK_a values. According to Seung-Jang Lee et al [11] the Raman spectra reported by Huguenin et al [10] correspond to ellagic acid a gallic acid dimer.

2. Materials and methods

2.1. Materials

Solid gallic acid (97% purity) was purchased from Sigma-Aldrich. Two different crystalline structures were observed at the microscopy level (50×) and described as rods and amorphous, see Fig. 1. The following chemicals were used for the preparation of the silver nanoparticles colloidal solutions: silver nitrate 99.9999% metal basis (Aldrich), sodium hydroxide (ACS, Reag. Ph Eur Merck) and hydroxylamine hydrochloride, 99.999% metal basis (Aldrich). All these chemicals were used as received.

2.2. Sample preparation for the Raman and SERS measurements

Raman measurements were performed for the gallic acid crystals deposited on a quartz slide and in aqueous solution according to a methodology described in one of our previous works [12]. To obtain the Raman spectrum in aqueous solution, a GA aqueous solution close to 0.10 M was prepared. For the SERS measurements, stock aqueous solutions of the analyte were prepared in ultrapure water, to a final concentration of 1.0×10^{-3} M. A low charged Ag colloidal solution was used; this is the same recently prepared giving excellent SERS results when working with large-electron systems [6]. To obtain the SERS spectra in dried samples an aliquot (10 μL) of the aqueous solution of the analyte is deposited on a quartz slide and the water is allowed to evaporate at room temperature. After that, the colloidal AgNps solution (20 μL) is dropped onto the dried analyte, thus obtaining the gallic acid AgNps aggregate in aqueous medium. The excess water is evaporated at room temperature and the dry sample is used for the SERS measurements.

2.3. Raman and SERS measurements

The SERS measurements were performed using a Renishaw micro-Raman RM 1000 spectrometer, equipped with laser lines 514, 633 and 785 nm. The spectrometer is coupled to a Leica microscope DMLM and a CCD camera electrically cooled. The Raman signal was calibrated to the 520 cm^{-1} line of silicon and lens of 50× objective. The laser power on the sample is about 0.2 mW. Acquisition time was set between 10 and 20 s per accumulation; the average of accumulations was 5 with spectral resolution of 4 cm^{-1}. The spectra were recorded between 100 and 1800 cm^{-1}. Spectral recording conditions and the choice of the laser line to be used is selected in order to avoid degradation of the sample; in this sense, the 633 and 785 nm laser lines were used.

3. Results and discussion

3.1. Computational details

Molecular geometry optimization, molecular electrostatic potential (MEP) and vibrational spectra calculations were performed for GA with the program package Gaussian 03 [13]. Density functional theory (DFT) with the B3LYP functional [14,15] were used for the optimizations of the ground state geometries and simulation of the vibrational spectra. The default convergence criteria and integration grid of the program were used. The basis set was the 6-311G [16]. Vibrational spectra were obtained without anharmonic corrections and Raman activities were determined using numerical differentiation.

The dominant character of each normal mode was determined by analyzing current assignments reported in the literature for the distinct functional groups present in GA, visual inspection of the atomic displacement of normal modes [17] as well as regarding the potential energy distribution matrix (PED) obtained from the multiple scale factors applied to different internal coordinate force constants, according the treatment proposed by Pulay et al. [18] which automatically scale the off diagonal force constants to offset the systematic error produced on the theoretical frequencies [19]. Transformation of Gaussian Cartesian force constants into the corresponding internal ones, conversion from Cartesian to internal coordinates, automatic generation of the redundant internal coordinates, SQM (Pulay) scaling, least-squares refinement of scale factors, and decomposition of the potential energy distribution (PED) were carried out using the program FCART01, a major modification of previous software [20] written to accomplish all the necessary transformation and calculations using the Gaussian output.

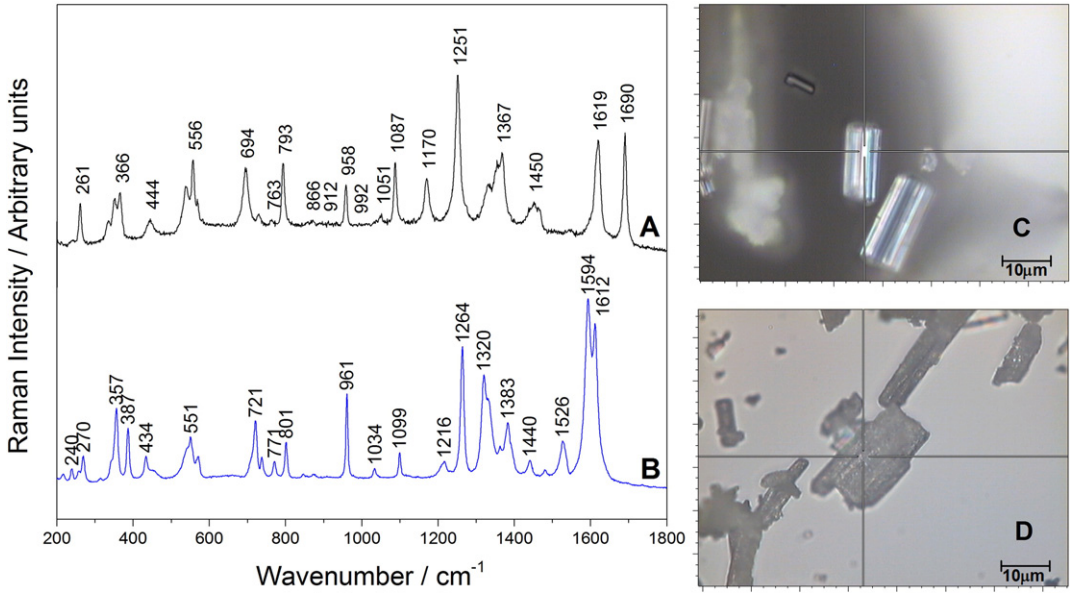

Fig. 1. Raman spectra of gallic acid crystals (dimer) (A) and gallic acid crystals (monomer) (B), laser line 785 nm. The right images show the crystals of GA dimer (C) and GA monomer (D) under a microscope using the 50× objective lens.

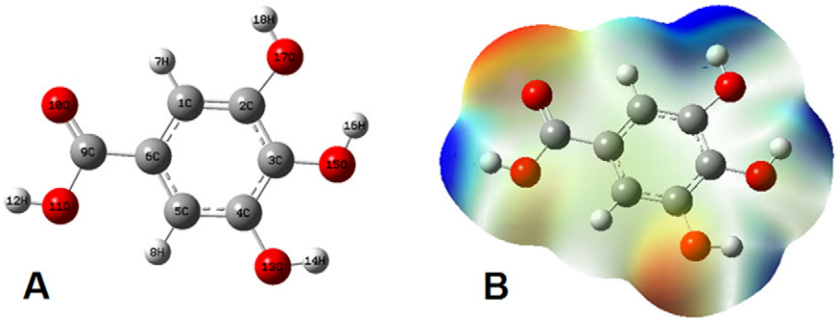

Fig. 2. B3LYP/6-311G-optimized structure of GA (A) and molecular electrostatic potential (MEP) contour of GA (B).

3.2. Optimized structure

The optimized geometry of GA calculated at our level of calculation is shown in Fig. 2A. At the optimized structure no imaginary frequency modes were obtained, proving that a local minimum and not a saddle point of the potential energy surface was found. Geometrical parameters of GA obtained at our level of theory are in agreement with those pointed out by X-Ray diffraction study [21] for the anhydrous molecule, being its structure essentially planar; geometrical parameters compared with those presented in reference [21], are included as Supplementary material. The Cs symmetry of the molecule with coplanar orientation of OH bond with the benzene ring supply unique information on the extent of symmetry lowering of benzene normal modes.

3.3. Molecular electrostatic potential (MEP) maps

MEP calculated at the B3LYP/6-311G-optimized geometry is presented in Fig. 2B. This map allows us to visualize variably charged regions of a molecule, indicating the most probable interaction of a charged point-like species on organic molecules [22], and consequently, giving insight on the nature of the chemical bond [23]. The different values of the electrostatic potential at the surface are represented by different colors. The color code of these maps is in the range between deepest red and deepest blue in the compound. The positive (blue) regions of MEP are related to nucleophilic reactivity, while the negative (red and yellow) regions of MEP are an indication of electrophilic reactivity, and green color represents regions of very low or zero potential.

3.4. Vibrational analysis

GA consists of 18 atoms with a total of 48 nonredundant coordinates. Bands concerning to Raman normal modes have been selected from the vibrational data according their intensity presented in the Gaussian output. In general, our results are similar to those presented in a previous DFT vibrational study where a different level of calculation was used (Becke3P86 functional and the 6-311G(d,p) basis set) [24]. Also, they can be can be compared to those obtained for related molecules, such as benzoic acid [25] and phenol [26,27].

After analyzing our results and comparing them with those obtained in previous calculations, it is noted that phenyl stretching vibrations are strongly associated to the CH in plane bending modes and the in plane ring deformations do not include the symmetric breathing fundamental as a consequence of the phenyl complexation. Furthermore, bands concerning hydroxyl and benzoic normal modes are located in well-defined positions in the spectrum, while ring vibrations are spread out in a wide spectral range. Specifically, the carbon–carbon stretching modes of the phenyl group are expected in the range from 1650 to 1200 cm^{-1}, however, It has been recognized that the actual position

Table 1
Selected calculated and experimental Raman and SERS wavenumbers (cm^{-1}) with relative intensities of GA and the most probable bands assignment.

Calc. SQM scaled	Raman solid sample	Raman aq. solution	Raman dimer	SERS	Assignment
1688		1688 bw	1690 s		92% νCO
1612	1612 vs	1619 vs	1619 s	1614 s	70% νCC ring + 25% νC-OH
1603	1594 vs				45% νCC ring + 39% δ C-H
1526	1526 m			1506 vw	51% νCC ring + 36% δ C-H
1466		1465 m			61% νCC ring + 27% νC-OH
1436	1440 w		1450 w	1430 vw	46% νCC ring + 28% νCO + 21% δOH
1364	1383 m		1367 m	1368 s	39% νCC ring +28% δCH + 27% νCOOH
1325	1320 s	1337 s		1311 w	42% νCC ring + 31%νCO + 22% νC-OH
1277	1264 vs	1257 w	1251 vs	1265 m	75% ρCO
1219	1216 vw				72% δOH (—COOH)
1179		1157 w	1170 m		56% δ C = O + 28% δCH
1108	1099 m	1105 w	1087 m	1096 w	69% δOH
1054	1034 vw	1045 vw	1051 vw	1047 vw	63% ipd ring
988		1002 vw			59% ipd + 35% ring νCO
944	961 s	963 m	958 m	961 w	76% ρCH *asym*
894		845 w			81% ρCH *sym*
871	801 m	810 m	793 m	797 m	88% ρCH *sym*
778	771 w				85% νCC + 10% δCO
760	721 m	711 s	694 m	710 m	76% τ CO
560	551 m	542 s	556 m	542 w	66% δCOH + 28% δring
448	434 w	452 vw	444 w	437 vw	72% ρring
410	387 m	398 w			65% τring
343	357 m	355 w	366 m	358 m	73% τring

Abbreviations: ν, stretching; δ, deformation; ρ, out of plane bending; τ, torsion; ipd, in plane deformation; *sym*, symmetric; *asym*, antisymmetric.
*Relative intensity: b, broad; vs, very strong; s, strong; m, medium; w, weak and vw, very weak.

of these modes are determined not so much by the nature of the substituents but by the form of substitution around the ring [28]. In Table 1 unscaled DFT and calculated multiple scaled frequencies, as well as the positions of Raman and SERS peaks and their vibrational assignments are collectively summarized. For the sake of brevity, this table just presents assignments concerning the most singular normal modes of GA, that is, those in the region between 1600 and 400 cm^{-1}.

3.5. Raman spectrum of gallic acid crystals

The Raman spectrum Fig. 1B of the amorphous crystals Fig. 1D, is coincident with published data of gallic acid by D. Kurouski et al [29]; these authors utilized tip-enhanced Raman scattering (TERS) to identify indigo dye and iron gall ink in situ on Kinwashi paper. The present proposed spectral assignment is based on our calculations as well as on previous data for the gallic acid [1,24,29] and characteristic group frequencies [30,31]. A confident bands assignment is relevant to a correct interpretation of the SERS spectrum; then, conclusions about the molecular orientation of the analyte on the surface can be adequately proposed. The Raman spectrum Fig. 1A of the rod crystals Fig. 1C, is highly consistent with a dimeric form of the gallic acid, involving the carboxylic fragment. This proposition is consistent with Raman data and DFT calculations by Seung-Jang Lee et al [11]. The present results suggest that the dimeric form corresponds to the ellagic acid. In fact, the band at 1690 cm^{-1} is a νCO mode characteristic of a ketone group [32,33] discarding an ester formation; for an ester, the carbonyl group displays a signal above 1735 cm^{-1}. Alvarez-Ros et al [3] reported the Raman spectrum of GA in ethanol; the reported bands are highly consistent with a dimeric form of GA. The dimer presence also involves severe spectral modifications in the 1300–1200 cm^{-1} region where the νC-O modes are active. Ring vibrations mainly bands ascribed to νCC (1526 cm^{-1}), asymmetric in plane deformation (1034 cm^{-1}) and out of plane deformation (387 cm^{-1}) are particularly sensitive to the dimeric structure. Table 1 contains the spectral assignment of both structures. The monomer dominates the Raman spectrum in water solution at pH 7.

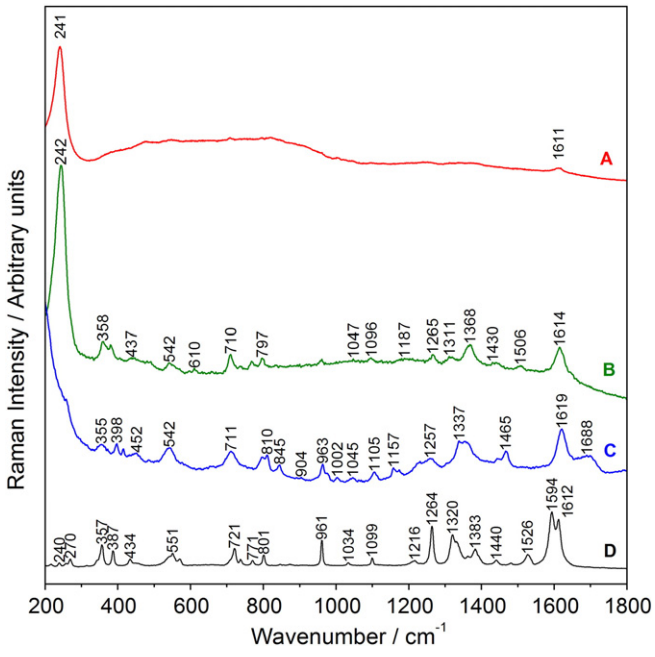

Fig. 3. SERS spectra of GA using the Leopold-Lendl Ag colloid (A) and from a modified Ag colloid (B), Raman spectra of GA in aqueous solution (C) and in solid (D). Spectra A, B and C were registered with the 633 nm laser line; spectrum D was registered with the 785 nm laser line.

3.6. SERS spectrum of GA in a dried system

The SERS spectrum of the gallic acid was not possible to obtain by using the Leopold-Lendl colloid [34], see Fig. 3A; the SERS spectrum in Fig. 3B was obtained in a dried system, by using the modified Ag colloid [6]. The SERS spectrum is compared with both the Raman spectrum of GA in solid and in aqueous solution, Fig. 3D and C, respectively. The comparison considers the spectrum of the monomer since this is the main species existing after dissolving the GA solid as deduced from the Raman spectrum of GA in solution (Fig. 3C).

The monomer structure dominates the SERS spectrum; this is based on the fact that both the SERS and the Raman signals of the monomer are nearly equivalents (Fig. 3B and D), displaying a similar spectral profile and consistent in both cases with a nonionic form. Intensity changes by surface effect are interpreted on the basis of the SERS selection rules [7]. Thus, it is possible infer about the orientation and organization of analytes on a metal surface. The spectral shifting observed by surface effect for some bands is related to a probable electronic charge transfer resulting from the ligand metal surface interaction. In the present case, no bands appear by surface effect and the general spectral shift is rather moderate which suggest that the analyte surface interaction is feeble. The relative intensity of the aromatic stretching νCC bands at about 1600 cm^{-1} in the Raman keep a comparative relative intensity in SERS solid; this is interpreted in terms that these vibrations correspond to a molecular aromatic fragment not plane parallel to the surface; an increasing of those bands should suggest a perpendicular position of the corresponding bonds. On this basis it is proposed a rather tilted orientation of the aromatic moiety on the surface. The Raman band at 1526 cm^{-1} ascribed to an aromatic νCC mode is observed in SERS at 1506 cm^{-1} keeping the same relative intensity; this is consistent with the above proposition but for a CC bond closest to the surface. The Raman band at 1440 cm^{-1} is assigned to a coupled νCO/νCC mode and an OH deformation of the carboxylic group; by assuming that the carboxylic moiety is nearly coplanar to the benzene ring, the COOH should be also tilted to the surface; the wavenumber shift to 1430 cm^{-1} in SERS suggests that the carboxylic group and at least one of the OH function are close to the surface. The multiple bands at 1383 and 1320 cm^{-1} are ascribed to coupled vibrations including the νCC, δCH and δOH modes following the calculations by Mohammed-Ziegler et al [24] and our theoretical results including a contribution of a νCOOH mode; these bands coalescent into a broad band at 1368 cm^{-1} in SERS. This spectral behavior is in the same sense of a tilted orientation while the wavenumber shift suggests an electronic redistribution of a molecular aromatic fragment close to the surface. The fact that the band at 1311 cm^{-1} probably due to a carboxylic νCO mode and observed only in the SERS spectrum, is associated to a nearly perpendicular position of the corresponding bond close to the surface. Since the medium relative intensity it is not discarded that this mode could belong to a ring CO bond of a whole molecular system tilted to the surface. The relative intensity of the strong Raman band 1264 cm^{-1} assigned to an out of plane C═O vibration (ρCO) drastically decreases by surface effect; this indicates that the C═O bond is not close to the surface and/or the carboxylic moiety is confirmed to be also tilted on the surface. This mode has the induced dipole nearly parallel to the surface. The weak Raman band at 1216 cm^{-1} is not observed in SERS; it is a carboxyl δOH mode. A similar situation occurs for the band at 1099 cm^{-1} due to a ring δOH mode. The polarizability *z*-component of these vibrations is decidedly not parallel to the incident laser excitation. The band at 961 cm^{-1} is observed with a weak relative intensity in SERS; this spectral situation and assuming a tilted orientation of the whole molecule on the surface suggests that this δCO mode belong to the carboxyl moiety in agreement with the calculations. If the band at 961 cm^{-1} is assigned to a ρCH mode, then the structural fragment associated should be plane

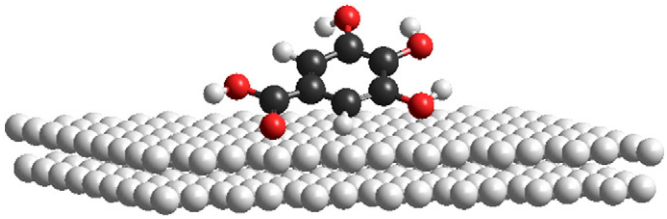

Fig. 4. Scheme of the gallic acid interacting with the Ag metal surface.

to the surface; however, the weak intensity supports the idea of an inclined system. This proposition is supported by the spectral behavior of the ρCH band at 801 cm^{-1} which keeps its relative intensity in SERS. This is also observed in the case of the band at 771 cm^{-1} which resulted from coupled νCC and δCO modes; it is observed weak in SERS. The CO torsion at 710 cm^{-1}, should belong to the carboxyl moiety if the orientation is that here proposed; this assignment is in agreement with that obtained from the potential energy distribution calculation. The band at 551 cm^{-1} maintains its intensity and is assigned to C—OH and ring deformations; this supports the idea of a not exactly coplanar orientation of the gallic acid on the surface. Bands below 440 cm^{-1} are ascribed to in and out of plane ring deformations; these bands are also observed in SERS which is only consequence of a rather tilted orientation of the molecule on the metal surface. Fig. 4 represents the proposed gallic acid metal surface interaction. The inferred position of GA on the surface is in concordance with the MEP contour obtained from DFT calculations (Fig. 2) where it is observed that the negative charge substantially covers the hydroxyl (O13) and carboxylic groups, that is, the more electronegativity of these groups makes then the most reactive part in the molecule.

4. Conclusions

Amorphous and rod crystals from a p.a. commercial product of gallic acid were microscopically separated. The Raman spectral analysis of the amorphous crystals suggests a monomeric form, while the rod crystal corresponds to a dimeric species, probably the ellagic acid. The dimer structure involves the carboxyl and hydroxyl moieties. Raman data indicate that the monomeric species dominates in water solution. A low negatively charged Ag colloid allowed obtain to the best of our knowledge, the first surface enhanced Raman scattering (SERS) spectrum of the gallic acid. SERS selection rules allowed propose an orientation of the analyte on the metal surface; a tilted orientation is inferred for the dried analyte on the surface. Comparison of Raman and SERS spectra suggests a tilted orientation of the benzene ring on the surface. Further, MEP contour has been useful to support both the assignment and the orientation of GA on the Ag nanoparticles. From this study it is possible to appreciate the effectiveness of the modified Ag colloid as a good surface to enhance the Raman signals. In order to interpret the advantages of the here used modified Ag colloid into obtain SERS data of high negatively charged analytes, a SERS study of the GA in solution along with a molecular dynamic interpretation are in progress in our laboratories.

Supplementary data to this article can be found online at http://dx.doi.org/10.1016/j.saa.2016.03.028.

Acknowledgments

Authors acknowledge project Fondecyt 1140524 from CONICYT. GDF thanks to DGI 01-1415 Universidad de Playa Ancha. CGL thanks project 3160252 from Fondecyt.

References

[1] A.S. Lee, P.J. Mahon, D.C. Creagh, Vib. Spectrosc. 41 (2006) 170–175.
[2] M. Leona, J. Stenger, E. Ferloni, J. Raman, Spectroscopy 37 (2006) 981–992.
[3] M.C. Álvarez-Ros, S. Sánchez-Cortés, O. Francioso, J.V. García-Ramos, J. Raman, Spectroscopy 32 (2001) 143–145.
[4] B. Imelik, C. Naccache, G. Coudurier, H. Praliaud, P.Meriaudeau, P. Gallezot, G. A. Martin, J. C. Vedrine (Eds.), Studies in Surface Science and Catalysis, Metal-Support and Metal-additive Effects in Catalysis, Elsevier, vol. 11 (1982).
[5] G. Diaz Fleming, U. Martinez, M. Mallea, J. Guerra, J. Spectrosc. Dyn. 4 (2014) 16.
[6] C. Garrido, Boris E. Weiss-López, M.M. Campos Vallette, Spectrosc. Lett. 49 (2016) 11–18.
[7] M. Moskovits, Rev. Mod. Phys. 57 (1985) 783–826.
[8] P. Kambhampati, C.M. Child, M.C. Foster, A. Campion, J. Chem. Phys. 108 (1998) 5013–5026.
[9] P. Hohenberg, W. Kohn, Phys. Rev. 136 (1964) 864–871.
[10] J. Huguenin, S.O.S. Hamadya, P. Boursona, J. Raman, Spectroscopy 46 (2015) 1062–1066.
[11] S.J. Lee, B.S. Cheong, H.G. Cho, Bull. Kor. Chem. Soc. 36 (2015) 1637–1644.
[12] C. Garrido, T. Aguayo, E. Clavijo, J.S. Gómez-Jeria, M.M. Campos-Vallette, J. Raman, Spectrosc. 44 (2013) 1105–1110.
[13] M.J. Frisch, G.W. Trucks, H.B. Schlegel, G.E. Scuseria, M.A. Robb, J.R. Cheeseman, J.A. Montgomery, T. Vreven, K.N. Kudin, J.C. Burant, J.M. Millam, S.S. Iyengar, J. Tomasi, V. Barone, B. Mennucci, M. Cossi, G. Scalmani, N. Rega, Petersson GA, H. Nakatsuji, M. Hada, M. Ehara, K. Toyota, R. Fukuda, J. Hasegawa, M. Ishida, T. Nakajima, Y. Honda, O. Kitao, H. Nakai, M. Klene, X. Li, J.E. Knox, H.P. Hratchian, Cross JB, V. Bakken, C. Adamo, J. Jaramillo, R. Gomperts, R.E. Stratmann, O. Yazyev, A.J. Austin, R. Cammi, C. Pomelli, J.W. Ochterski, P.Y. Ayala, K. Morokuma, G.A. Voth, P. Salvador, J.J. Dannenberg, V.G. Zakrzewski, S. Dapprich, A.D. Daniels, M.C. Strain, O. Farkas, D.K. Malick, A.D. Rabuck, K. Raghavachari, J.B. Foresman, J.V. Ortiz, Q. Cui, A.G. Baboul, S. Clifford, J. Cioslowski, B.B. Stefanov, G. Liu, A. Liashenko, P. Piskorz, I. Komaromi, Martin RL, Fox DJ, T. Keith, M.A. Al-Laham, C.Y. Peng, A. Nanayakkara, M. Challacombe, P.M.W. Gill, B. Johnson, W. Chen, M.W. Wong, C. Gonzalez, J.A. Pople, Gaussian 03, Revision C.02, 1, Gaussian, Inc., Wallingford CT, 2004.
[14] A.D. Becke, J. Chem. Phys. 98 (1993) 5648–5652.
[15] C. Lee, W. Yang, R.G. Parr, Phys. Rev. B Condens. Matter 37 (1988) 785–789.
[16] R. Ditchfield, W.J. Hehre, J.A. Pople, J. Chem. Phys. 54 (1971) 720–723.
[17] A. Frisch, A.B. Nielsen, A.J. Holder, GAUSSVIEW Users Manual, Gaussian Inc, 2000.
[18] P. Pulay, G. Fogarasi, F. Pang, J.E. Boggs, J. Am. Chem. Soc. 101 (1979) 2550–2560.
[19] J.B. Foresman, A. Frisch, Exploring Chemistry with Electronic Structure Methods, second ed. Gaussian Inc., Pittsburgh, PA, 1996.
[20] W.B. Collier, QCPE Bull. 13 (1996) 16502.
[21] J. Zhao, I.A. Khan, F.R. Fronczek, Acta Cryst. 67 (2011) 316–317.
[22] G. Naray-Szabo, G.G. Ferenczy, Chem. Rev. 95 (1995) 829–847.
[23] J.S. Murray, K. Sen, Molecular Electrostatic Potentials, Concepts and Applications, Elsevier, Amsterdam, 1996.
[24] I. Mohammed-Ziegler, F. Billes, J. Mol, Struct. (Theochem.) 618 (2002) 259–265.
[25] G. Keresztury, F. Billes, M. Kubinyi, T. Sundius, J. Phys. Chem. A 102 (1998) 1371–1380.
[26] Y.J. Kwon, D.H. Son, S.J. Ahn, M.S. Kim, K. Kim, J. Phys. Chem. 98 (1994) 8481–8487.
[27] D. Michalska, D.C. Bienko, A.J. Abkowicz-Bienko, Z. Latajka, J. Phys. Chem. 100 (1996) 17786–17790.
[28] L. J. Bellamy, John Wiley & Sons Inc. New York, 1975.
[29] D. Kurouski, S. Zaleski, F. Casadio, R.P. Van Duyne, N.C. Shah, J. Am. Chem. Soc. 136 (2014) 8677–8684.
[30] D. Lin-Vien, N.B. Colthup, W.G. Fateley, J.G. Graselli, The Handbook of Infrared and Raman Characteristic Frequencies of Organic Molecules, Academic Press, Boston, 1991.
[31] G. Socrates, Infrared and Raman Characteristic Group Frequencies, Tables and Charts, John Wiley & Sons, Chichester, 2001.
[32] Y. Tao, Z.A. Dreger, Y.M. Gupta, Vib. Spectrosc. 73 (2014) 138–143.
[33] N.F.L. Machado, R. Calheiros, A. Gaspar, J. Garrido, F. Borges, M.P.M. Marques, J. Raman, Spectroscopy 40 (2009) 80–85.
[34] N. Leopold, B. Lendl, J. Phys. Chem. B 107 (2003) 5723–5727.